

# International Conference on Space Optics—ICSO 2022

Dubrovnik, Croatia

3–7 October 2022

*Edited by Kyriaki Minoglou, Nikos Karafolas, and Bruno Cugny,*



## ***CHIME's Hyperspectral Imager (HSI): Status of Instrument Design and Performance at PDR***



## CHIME's Hyperspectral Imager (HSI): Status of Instrument Design and Performance at PDR

P. Buschkamp <sup>\*a</sup>, J. Hofmann <sup>a</sup>, D. Rio-Fernandes <sup>a</sup>, P. Haberler <sup>a</sup>, M. Gerstmeier <sup>a</sup>,  
C. Bartscher <sup>a</sup>, S. Bianchi <sup>b</sup>, P. Delpet <sup>b</sup>, H. Weber <sup>c</sup>, H. Strese <sup>c</sup>, J. Nieke <sup>c</sup>

<sup>a</sup> OHB System AG, Weßling - Oberpfaffenhofen, Germany;

<sup>b</sup> Thales Alenia Space, Cannes, France;

<sup>c</sup> European Space Agency (ESA), European Space Research and Technology Centre (ESTEC),  
Noordwijk ZH, The Netherlands

### ABSTRACT

CHIME, the Copernicus Hyperspectral Imaging Mission for the Environment, is one of six new missions that the EU and ESA are developing to expand the current suite of Copernicus Sentinels. The CHIME mission will provide systematic hyperspectral images to map changes in land cover and help sustainable agricultural practices. The contract for the development of two CHIME Satellites has been awarded in November 2020 to Thales Alenia Space France as Industrial Prime together with OHB Germany as Instrument Prime responsible for the novel Hyperspectral Imager (HSI). Compared to the two hyperspectral precursor missions, EnMAP (DLR) and PRISMA (ASI), CHIME will provide an enhancement allowing continuous and fully operational hyperspectral mapping of the Earth's surface.

The Hyperspectral Imager (HSI) on both satellites is a high-performance pushbroom imaging spectrometer type of instrument. Each instrument records ~130km of swath at 30m x 30m ground sampling. The spectral sampling interval is 10nm, covering a continuous spectral range from 400 nm to 2500 nm. A high performance Three Mirror Anastigmat (TMA) type telescope with wide-band coated optics collects the light reflected from ground and images it to three highly linear radiometric responsive and almost distortion-free spectrometers attaining very good spectral stability. All optical units are mounted to a torus-like carbon fiber (CFRP) optical bench structure providing the necessary line of sight stability. The electro-optical back end is based on passively cooled Teledyne CHROMA-D digital readout detectors creating robust margin in the predicted Signal-to-Noise performance. In flight, the HSI can be calibrated via on-board devices and using reference targets outside the spacecraft.

We present the design of the instrument payload at the stage of the Preliminary Design Review (PDR) mid 2022. We show the predicted instrument performance and discuss several design aspect highlights, like the carbon-fiber torus optical bench and the novel spectral calibration unit based on a combination of diffused sun illumination and absorption glass filters.

**Keywords:** Remote Sensing, Hyperspectral, Spectrometers, Free-form Optics

### 1. INTRODUCTION TO THE HYPERSPECTRAL IMAGER (HSI)

The main mission objective of the Copernicus Hyperspectral Imaging Mission is: “To provide routine hyperspectral observations through the Copernicus Programme in support of EU and related policies for the management of natural resources, assets and benefits. This unique visible-to-shortwave infra-red spectroscopy based observational capability will in particular support new and enhanced services for food security, agriculture and raw materials. This includes sustainable agricultural and biodiversity management, soil properties characterization, sustainable mining practices and environment preservation.”[4].

CHIME will provide an enhancement compared to the precursor missions EnMAP (DLR) [1] and PRISMA (ASI) [2], allowing to map the Earth's surface at less than 10 days revisit in a constellation of two spacecraft. The CHIME mission is designed for nominal routine operations of seven years with additional fuel for five years. The status of ongoing activities is reported in [3].

On-board of the two CHIME satellites, the Hyperspectral Imagers (HSI) will allow to acquire data with high spectral, spatial and radiometric quality. This data will have the potential to deliver significant enhancement in quantitative value-added products as required in the Mission Requirement Document [4].

\* peter.buschkamp@ohb.de; ohb-system.de

### Instrument Architecture

The underlying concept of the Hyperspectral Imagers (HSI) is that of a pushbroom imaging spectrometer. The instrument provides ~130 km of swath at 30 m ground sampling distance (GSD), employing spatial swath-splitting: To allow a high Signal to Noise ratio for the required GSD, a single (large aperture and) wide-field Three Mirror Anastigmat (TMA) telescope with a folding mirror after the third mirror (M3) was selected, feeding three independent identical full wavelength range VISIR grating spectrometer back ends in a staggered slit configuration. The telescope sizing is mostly governed by radiance levels, the physical size of the side by side staggered slits and the telescope's telecentric beam approach. The slit overlap ensures a seamless swath combination. The de-magnifying optical design allows the telescope to operate at a focal ratio of F5.5, relaxing tolerances and alignment, while the spectrometers are built in a more compact arrangement at moderate F3.3. The offner-type spectrometers employ dual-blazed curved gratings delivering 8.4 nm spectral sampling interval (SSI).

The instrument is built around a central torus-like hollow CFRP frame structure that provides the necessary opto-mechanical stiffness in a single element. The glass telescope mirrors mount directly to the central torus via CFRP support structures. The star trackers are attached to the main torus via a combined CFRP-Invar Interface. At the focal plane of the telescope, the three identical spectrometer units (an all-aluminium design) mount to a common aluminium spectrometer support structure that connects to the central optical frame torus from below via blades for the necessary thermoelastic isostatic decoupling. This arrangement keeps the center of gravity (CoG) close to the platform and significantly facilitates assembly, integration, test (AIT) and verification efforts.

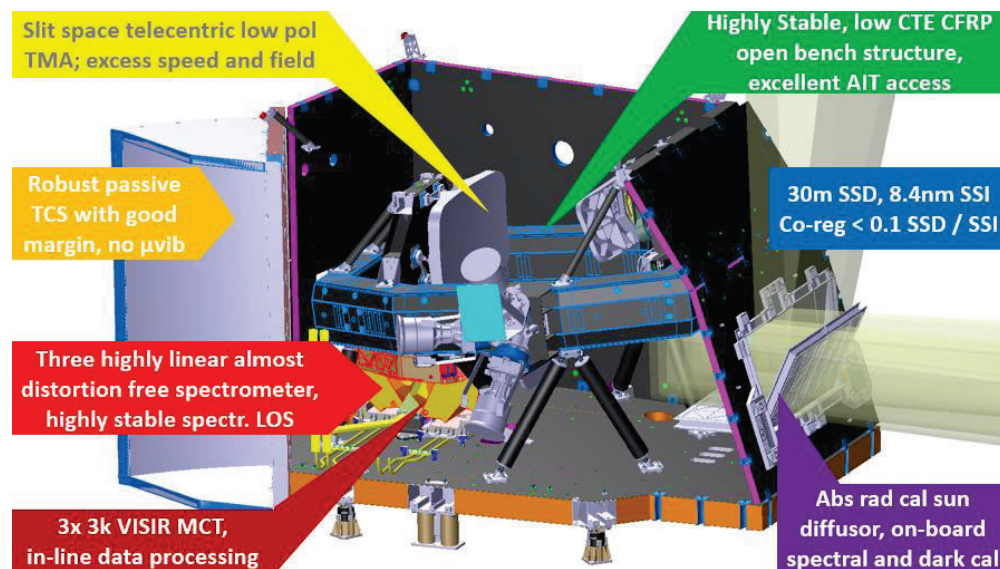


Figure 1. CHIME Instrument Key features (Some CAD elements removed to show a better overview)

All units, except the three MCT detectors, that mount to the three spectrometers work at ambient temperature. The temperature controlled single material (AlSi) spectrometers with wide-band gratings are fed by a wide-field Three Mirror Anastigmat (TMA) telescope with wide-band UV-enhanced Zerodur mirrors and a folding mirror to compact the instrument. The three cold (~175 K) detection back ends are built around the digital-readout Teledyne CHROMA-D MCT 3k detectors. Each of the three detectors has the size of 3072x512 pixels representing the spatial and full VIS-SWIR spectral dimension respectively. The pixels are binned 2x2 to increase SNR. Both, the slit limited SSI of 8.4 nm and the 30m spatial sampling distance (SSD) are Nyquist sampled before binning and can be transferred unbinned for instrument checks or calibration. The thermal control system (TCS) builds on a robust passive cooling chain with margin using a single two-stage radiator with CPC reflector to cold space. The instrument supports calibration via reference targets (solar absolute radiometric calibration, spectral calibration source) and vicarious calibration via proxy targets (ground, moon, and atmosphere).

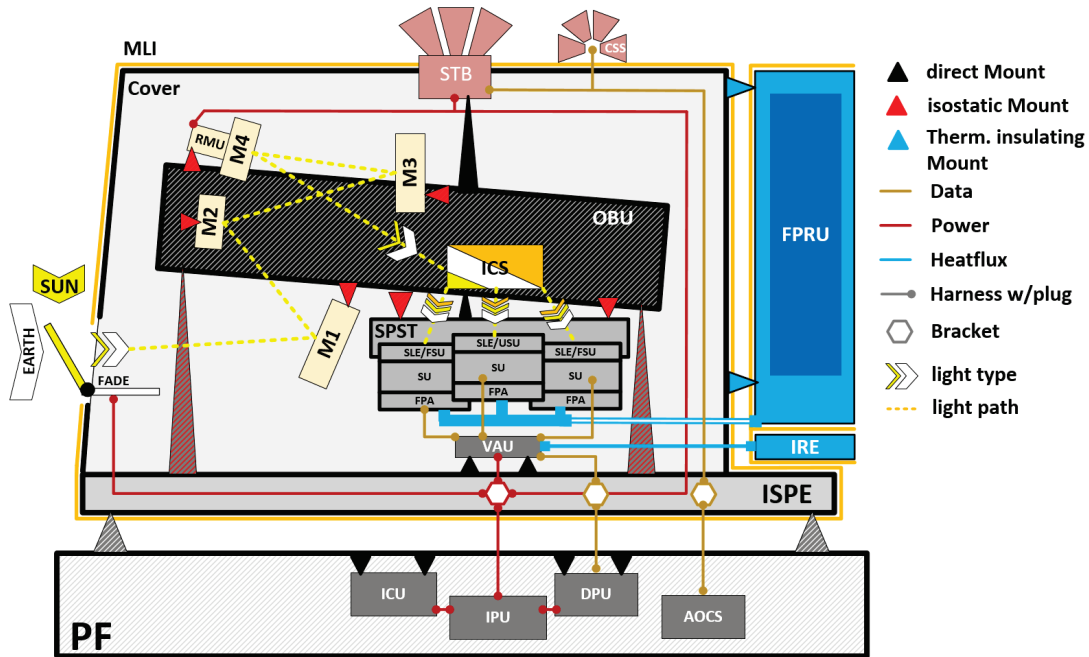


Figure 2. Instrument layout (Abbreviations see Figure 4)

Figure 2 shows the conceptual layout of the instrument. It shows the main entities and building blocks of the instrument in their relative/approximate spatial and in their functional arrangement.

The instrument is closed with a cover structure equipment (black line around the main parts in the sketch) and is covered in multi-layer insulation (yellow line). The radiators of the thermal control system are mounted on the cover on the outside of the instrument. Attitude control sensors like the Star trackers, are also fully or partly on the outside.

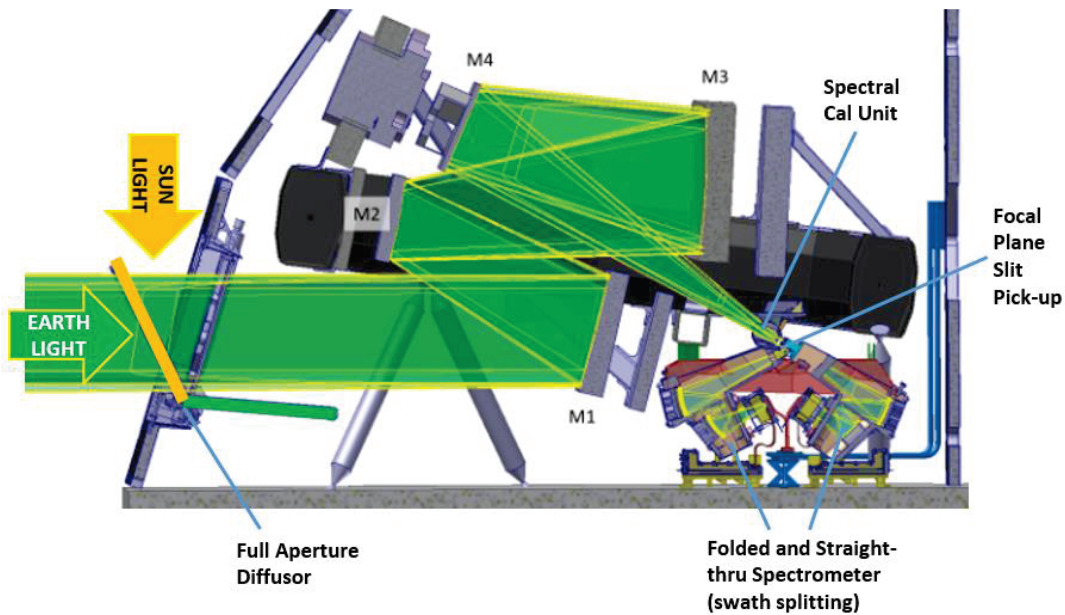


Figure 3. Instrument optical path, side view.

Figure 3 shows the optical path as a cut through the instrument CAD model. The Full Aperture Diffusor on the left can be deployed (orange line) for absolute radiometric sun calibration or stored (green line) during earth observation (EO). In EO mode, the diffusor faces the dark instrument panel and is protected from exposure to UV radiation. The spectrometers on the right form a very compact arrangement with short distance to the video acquisition units on the bottom and the detector cooling lines in between (blue "x") to reduce thermal parasitics.

For a deeper discussion of the optical layout, telescope, spectrometer and TCS aspects, we refer to our first paper [5]. In the following we report on the PDR designs of some of the instrument's systems that were introduced in [5] on a conceptual level.

## 2. OPTICAL BENCH AND INSTRUMENT STRUCTURE

All elements of the optical and electro-optical imaging chain are held by a central stiffness-providing element, a central CFRP torus (CFRP composite with no honeycomb core) creating an ultra-stable stiffness architecture for the instrument's structure. Having one central stiffness-providing element increases the predictability of the entire structural architecture and greatly improves the robustness of the instrument design.

All other instrument components are located around this torus, creating an overall very modular and accessible instrument design:

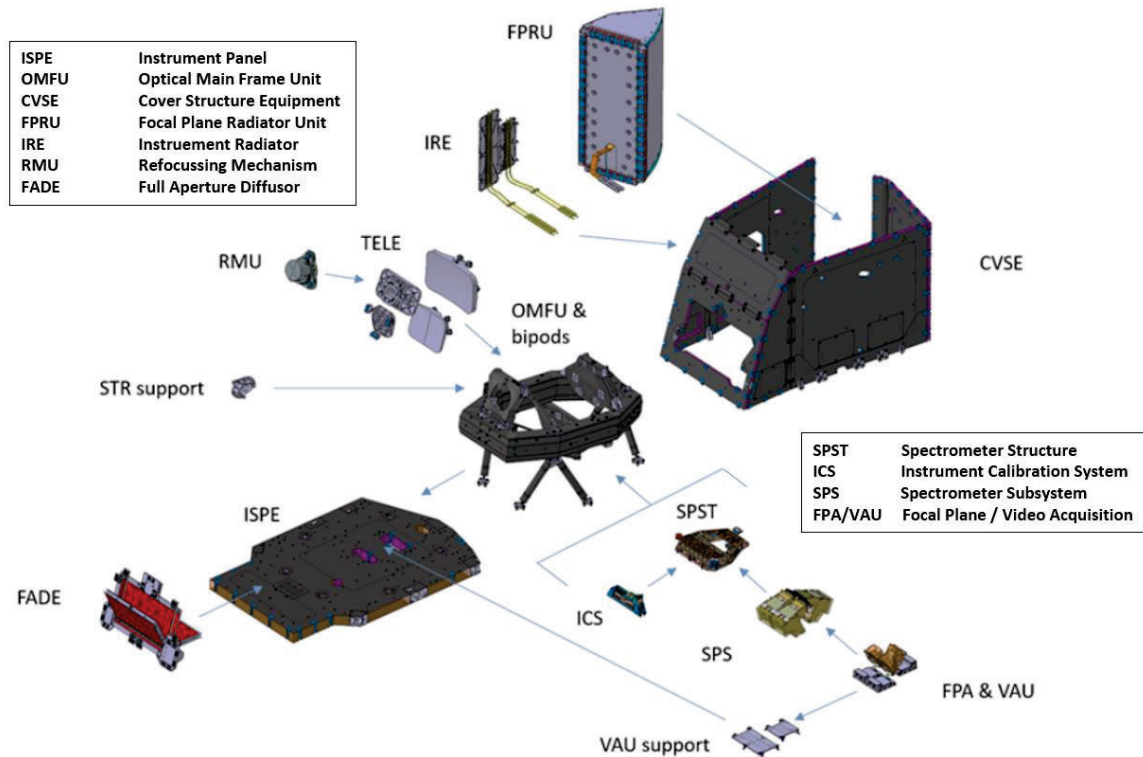


Figure 4. Instrument exploded view, MLI and Harness not shown



## 2.1 The Optical Bench Equipment (OBE):

The OBE consists of the Optical Main Frame Unit (OMFU), which is the Main Bench Torus (MBT) and dedicated support structures for the mirrors and refocus mechanism (TM1S to TM4S & RM4S) and the Optical Bench Isostatic Mounts (OBIM).

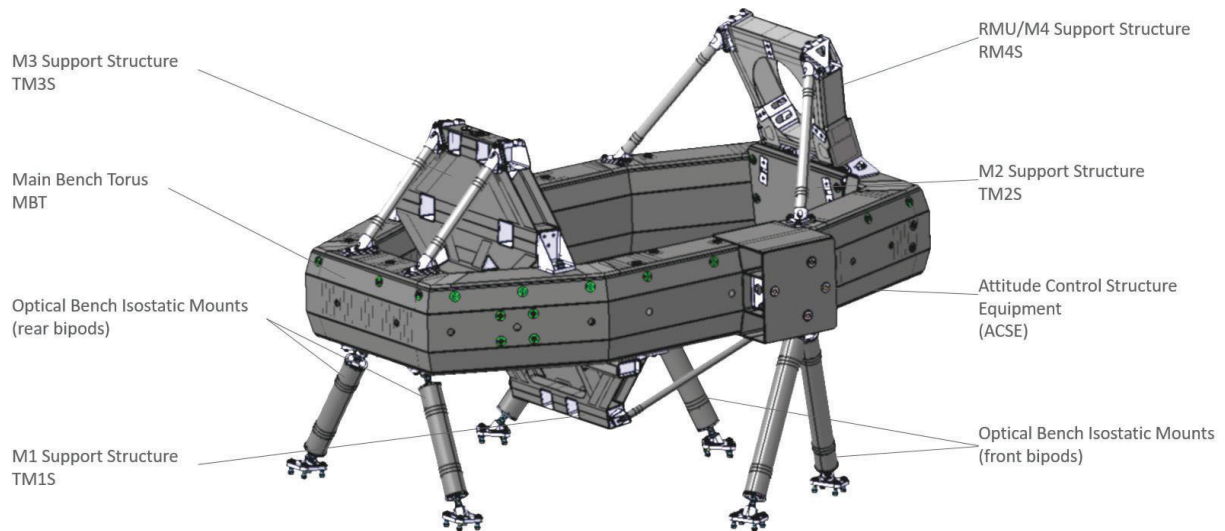


Figure 5. Close up view of the PDR design for the CFRP optical bench

The design concept for the OBE is based on a full CFRP structure architecture with metallic fittings and inserts. The MBT is a ring shaped CFRP structure built from high modulus fiber profiles to form a closed loop structure. To further increase the overall stiffness of the MBT, the torus is internally reinforced. The optical bench assembly is not a monolithic structure: The torus includes interface brackets to Bipods and Mirror Support Structures. All the mirror support structures are removable and attached to the MBT by fasteners to minimize the risks in case of damage.

The mirror support structures follow the same design principle as the Main Bench Torus, i.e. to build up a structure from CFRP profiles, where metallic brackets are used at the load introduction points.

The general manufacturing as well as assembling concept of the torus profiles has been investigated in a pre-development. FEM supported analysis confirm the structural integrity from a global point of view, further detailed design optimizations, for the local interface design and reinforcement have been performed to ensure structural design compliance at critical/high loaded interfaces (e.g. bipod interfacing area and mirror support structures interfacing area).

The OBE is enclosed in MLI. This creates a very stable thermal environment, leading to a very stable line of sight (see section 4.5) and also channels the water that is outgassing from the CFRP after launch.

## 2.2 Spectrometers and Spectrometer Structure

The spectrometers are an all-aluminium design. The necessary thermoelastic decoupling from the CFRP torus happens on the level of the spectrometer structure (SPST). All three spectrometers are mounted together onto one inverted cradle of the same material as the spectrometers. This creates a very compact spectrometer backend that ensures constant relative alignment of the three slits. The backend attaches to the torus behind Telescope mirror 1 and below Telescope Mirror 3 via blades for thermo-elastic decoupling. This means that the Video Acquisition units (VAU) can be located very close-by and the detector thermal control system (TCS) can be implemented with little parasitics.

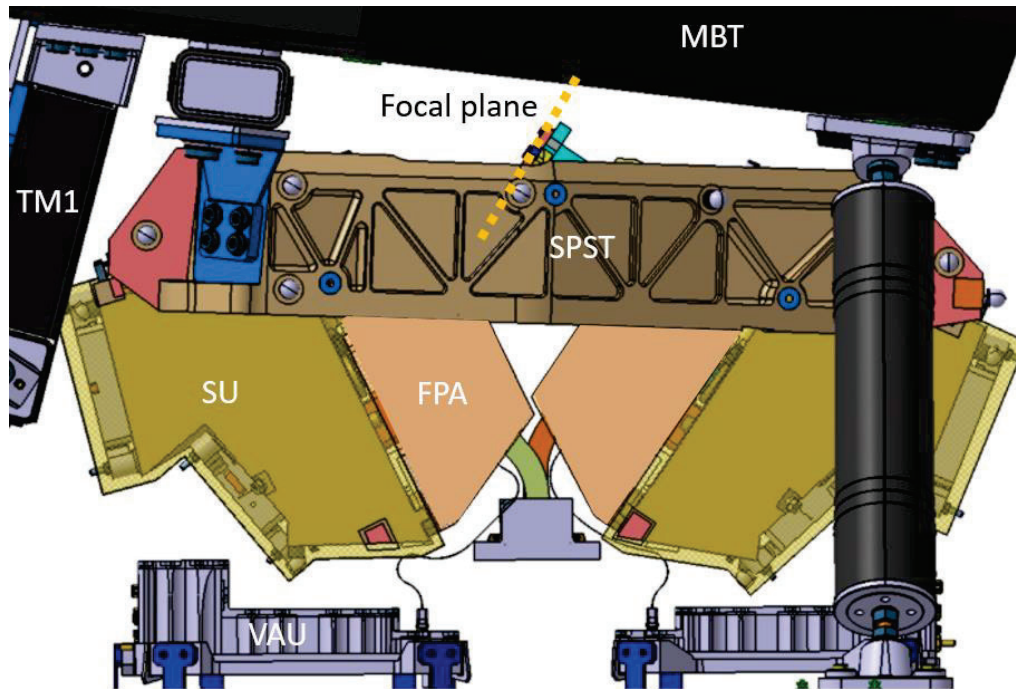


Figure 6. Spectrometer Structure (SPST) with the spectrometer units (SU) attached from underneath. The SPST (aluminum) to MBT (CFRP) connection is done via decoupling blades (blue). Cover MLI removed to show detail.

### 3. THERMAL CONTROL

The three Teledyne CHROMA-D detectors operate at  $\sim 175$  K to ensure the full performance over the full spectral range with cold-biased temperature control. The necessary cold sink is provided by a passive cryogenic radiator concept. It has been chosen over a mechanical cryo cooler for reliability, simplicity and absence of microvibration. Since CHIME operates in a low earth sun-synchronous orbit and maps the surface continuously, there exists a fixed cold-space-facing side on the payload at any time. Thus, a cold radiator facing cold space at all times can be mounted on the instrument.

#### 3.1 Thermal collector and Detector connection

The detectors are cooled via individual cold straps attaching to a common thermal collector and heatpipe interface offloading to a cryogenic two-stage radiator on the outside of the instrument. The compact arrangement of the spectrometers and the detector backend that “meet” back to back make very short paths possible significantly reducing parasitics.

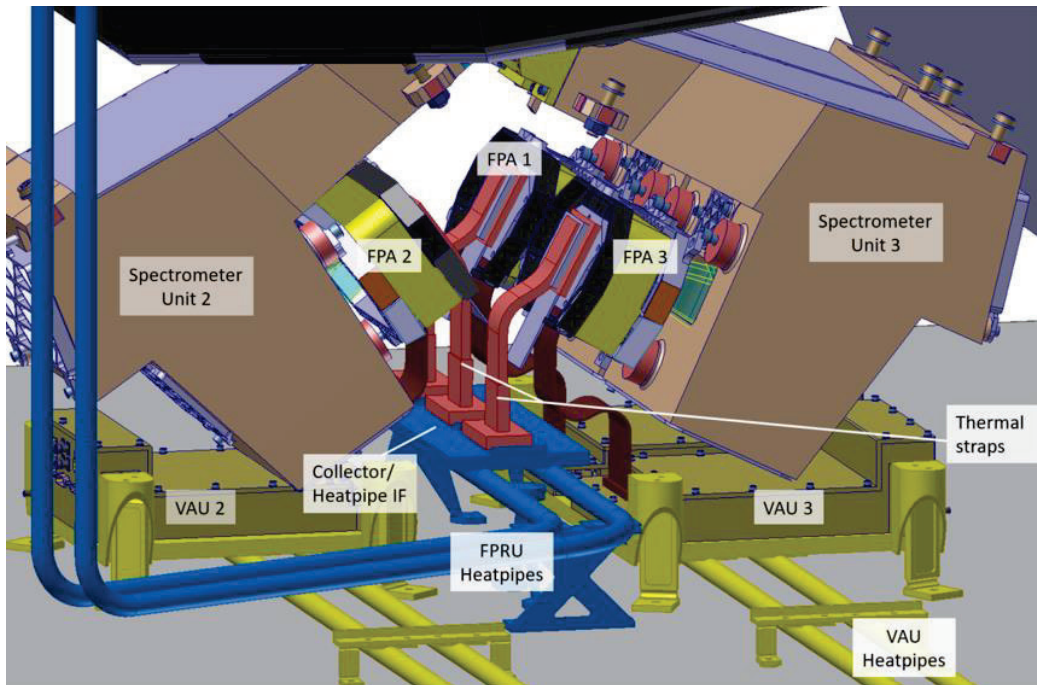


Figure 7. Detector Thermal control backend at the focal planes. SPST, Thermal covers and MLI removed to show detail.

### 3.2 Focal plane Radiator

The dedicated focal plane radiator is a two stage design. To offload the three detectors dissipation it is of considerable size and features a sun-shield with parabolic shape for increased coupling to cold space and efficient rejection of parasitics. Two cryogenic ethane heat pipes are used to couple the cold stage to the detectors.

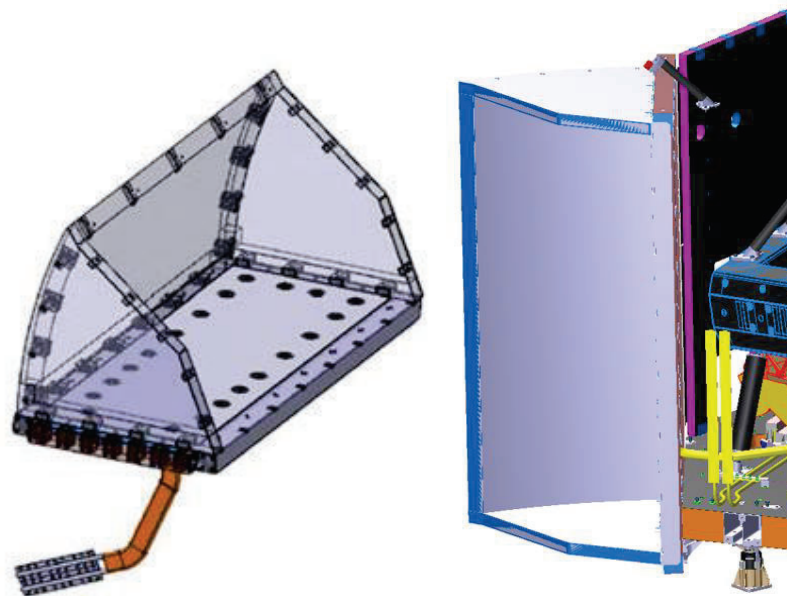


Figure 8. FPRU design (left) and location on the rear of the instrument (right, facing the space craft cold space side)



#### 4. INSTRUMENT PERFORMANCE

The Chime instrument is a high performance, hyperspectral pushbroom imaging spectrometer. Table 1 gives an overview of the main spatial and spectral performance indicators of the CHIME instrument. All numbers are confirmed by the PDR performance analysis.

Table 1: Instrument Key-Performance parameters

Parameter	Design Value	Comment
Spectral range	400 nm – 2500 nm	
Spectral resolution	< 11 nm	worst case at field of view edge
Spectral Sampling Interval (SSI)	8.4 nm	
Spectral Stability	< 0.2 nm	
Spatial Sampling Distance (SSD)	< 31 m	worst case at FoV edge
SNR	~300-400 up to 1350 nm ~> 200 up to 1750 nm ~50-150 up to 2500 nm	as CHIME has no fixed bands, see section 4.3, figure 10
MTF (@ Nyquist)	>0.25	valid for along- and across track direction (ACT and ALT)
Field of View (FOV) (Swath)	< 11.7° (~130 km)	full swath; three spectrometers
Keystone	< 0.07 pixel	binned pixel
Smile	< 0.07 pixel	binned pixel

The ground sampling distance is <31 m ACT (set by pixel size modulo distortion) and 30 m ALT (set by exposure time & slit width). The sampling slightly varies with the orbit. The optical performance measure for resolution dependent contrast, namely MTF at Nyquist frequency, is tailored to the requirement of >0.25 for ALT and ACT direction. The values consider a 2x2 binning of the detector pixels to improve the radiometric performance. The instrument allows also measurements with a different binning or with no binning for tests and calibrations (see detector read out mode section).

The spectral sampling interval (SSI) of 8.4 nm is adapted to the detector with 256 binned pixels. Thus, 250 pixels are required to cover the spectral range of 400 nm to 2500 nm. The oversizing of the detector by 6 pixels respects alignment margins and allows the usage of the edge pixels for background monitoring. The spectral resolution varies over the field of view and the wavelength range. Its performance calculation respects the detector effects, the slit width as well as the spectrometer effects. The spectral resolution is smaller than 11 nm for all areas. It improves towards the center of the field of view and spectral range, as it is affected by edge effects of the free-form mirrors of the spectrometer. In general, the performance of the spectral resolution is based on a careful optimization. Further improvement of the spectral resolution would be at the expense of spectrometer formed image distortion. Excellent Keystone and Smile performance is expected due to the combination of registration of the entire spectral range on a single detector and the low distortion of the optical path.

#### 4.1 Focal plane Layout - Swath spatial splitting, pixel usage

The instrument swath is governed by the instrument’s revisit requirement. The resulting swath of ~130 km combined with the required ground sampling distance of 30 m demands ~4300 detector pixel. To cover this, a staggered setup of three spectrometer and detector units (SU) is chosen. This makes it possible to use the existing high performance Teledyne e2V CHROMA-D detectors. The SUs are identical except for an additional folding-mirror in each of the two spectrometers that cover the left and right part of the swath for accommodation reasons. The SUs are arranged such that the “pick-off” slits that define the swath are positioned in the focal plane of the common front telescope, as shown in figure 9.

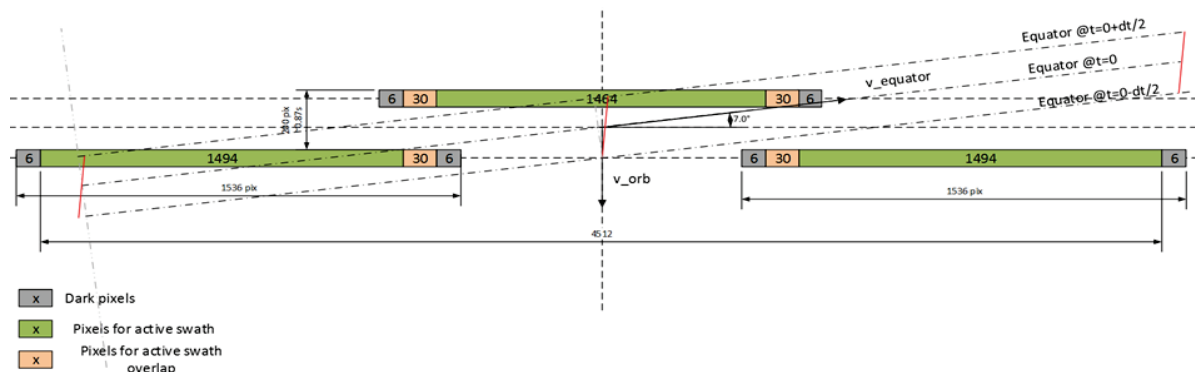


Figure 9. Pixel Layout in the staggered slit focal plane.

The offset arrangement in along track (= flight) direction, stems from the optical concept chosen for CHIME (see [5]). The spectrometers feature a de-magnification function that makes the spectrometers compact but relaxes the optical constraints put on the front-end telescope optics. (F3.3 in the spectrometers vs F5.5 in the telescope).

This arrangement provides the necessary mechanical accommodation clearance between the focal plane areas of the individual units (see [5]). The staggered slit layout in the telescope focal plane includes overlaps between the spectrometer slits that allow for cross calibration of the three data streams and places the slits in the areas of the telescope focal plane, which have an equally low wavefront error.

Each slit has a width corresponding to 1524 binned pixels on the detector. The overlap between the middle spectrometer and the respective outer spectrometer (for cross calibration) is 30 binned pixels. Additionally, the detector of each spectrometer has six binned pixels on each side, which are outside the area on which the slit is imaged. These non-irradiated “dark” pixels can be used for background monitoring. All irradiated non-overlapping detector pixels add up to 4512 binned ACT pixels satisfying the aforementioned need of more than 4300 across-track pixels creating the swath.

#### 4.2 Detector Readout modes

The detection system features several read-out modes as summarized in table 2. The nominal observation mode uses a 2x2 binning of the detector pixels. The geometrical calibration mode has no spatial binning but double spectral binning allowing a higher spatial performance while keeping the total pixel number constant. The further two detector readout modes, spectral calibration and detector calibration, use less binning than the nominal observation mode or no binning at all. This requires skipping of some iFOVs (limitation set by the instrument data rate) irrelevant for the modes’ usage.

The instrument design is tailored to the nominal observation mode. Thus, the slit of each spectrometer is imaged in two spectral pixels. The removal of spectral binning gives only a minor improvement of the instrument’s spectral resolution since the overall spectral resolution is slit limited.

Table 2. CHIME Instrument Detector Readout modes

Instrument Science data format	Detector pixel binning (Spatial direction)	Detector pixel binning (spectral direction)	# of skipped adjacent IFOVs along track*
Nominal (Earth) Observation**	2	2	0
Spectral calibration	2	no	2
Geometrical Calibration	no	2	0
Detector monitoring	no	no	4

\* Because of data transfer limitation set by data rate, this is no limitation for the intended operations

\*\* 2x2 binning used to increase SNR

### 4.3 Instrument SNR

The main radiometric performance figure is the signal to noise ratio (SNR), which is presented in figure 10, with the relevant radiance levels shown in figure 10a. The figure shows the signal to noise ratio of the PDR status for realistic worst-case assumptions for the detector performance. The realistic worst-case assumptions consider all bottom-up analysis available at PDR as well as assumptions on the detector read noise and quantum efficiency based on the detector pre-development phase.

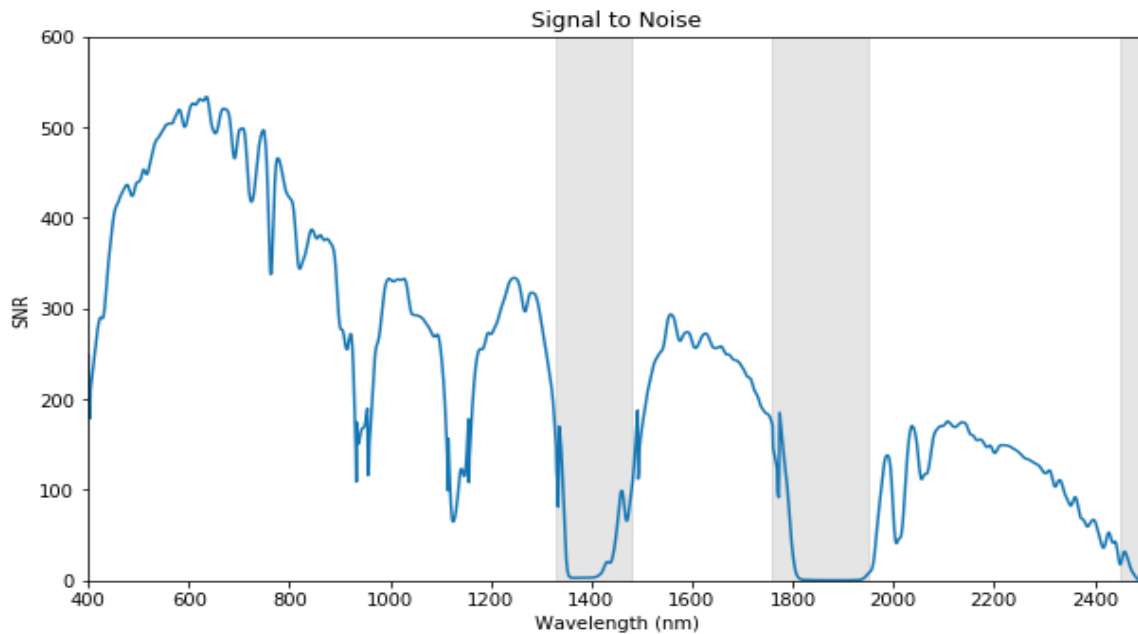


Figure 10. CHIME HSI Signal to Noise Graph; grey bars are exclusion zones (set by atmospheric absorption)

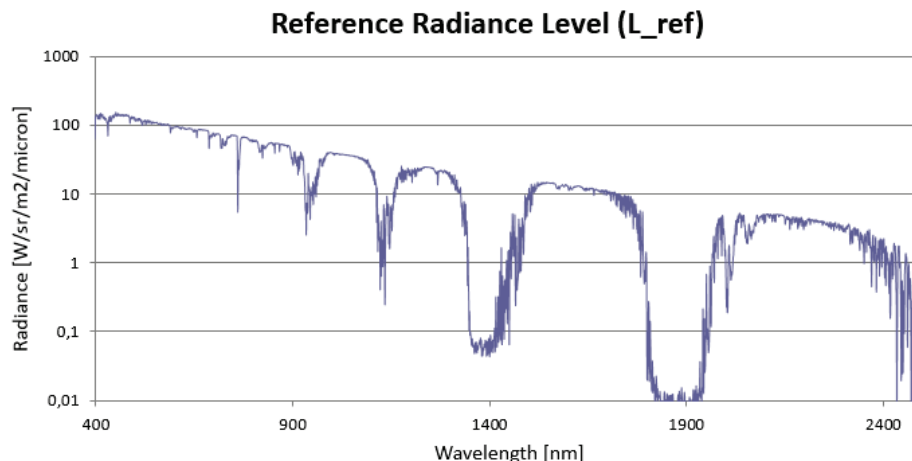


Figure 10a. CHIME HSI Reference Radiance  $L_{ref}$  to compute the SNR

The graph shows that the SNR in the VIS and NIR is better than 400 (excluding the blue edge of the wavelength range, where the SNR drops to 200). The SNR is still better than 200 for wavelengths up to 1750 nm. The grey areas in the plot mark the strongest atmospheric absorption bands with best-effort performance.

The general shape of the SNR follows the sun spectral radiance explaining the general drop of SNR performance towards higher wavelengths. The local drops of the SNR are caused by atmospheric absorptions bands, where the signal is low.

The good SNR performance is achieved by the usage of a dual blazed grating inside the spectrometers providing high grating efficiencies over the whole spectral range \*. Additionally, CHIME uses a customized Teledyne CHROMA-D MCT 3k detector with an adapted pixel full well capacity to minimize the read noise of the instrument.

\*Please refer to the ICSO 2022 paper “The Dual-blazed Diffraction Grating of the CHIME Hyperspectral Instrument: design, modelling & breadboarding” for more detailed information about the grating. [6]

#### 4.4 Radiometric Accuracies

The design achieves an absolute radiometric accuracy (ARA) of ~2% for most of the spectral range, as shown in figure 11 (status PDR assessments). The areas with less accuracy correspond to areas with strong atmospheric absorptions and low signals. Again, the grey parts of the plot mark the best effort areas. In contrast to the SNR plot, there is no exclusion area between 1330 nm and 1480 nm. Here, the radiance of cirrus clouds is assumed for calculation of the ARA. Frequent radiometric calibrations, using a sun diffusor, are planned to guarantee the absolute radiometric accuracy in orbit (see calibration section).

Overall, the instrument shows a high radiometric performance with an SNR ratio up to 500 and an ARA of 2% according to performance analysis for PDR.



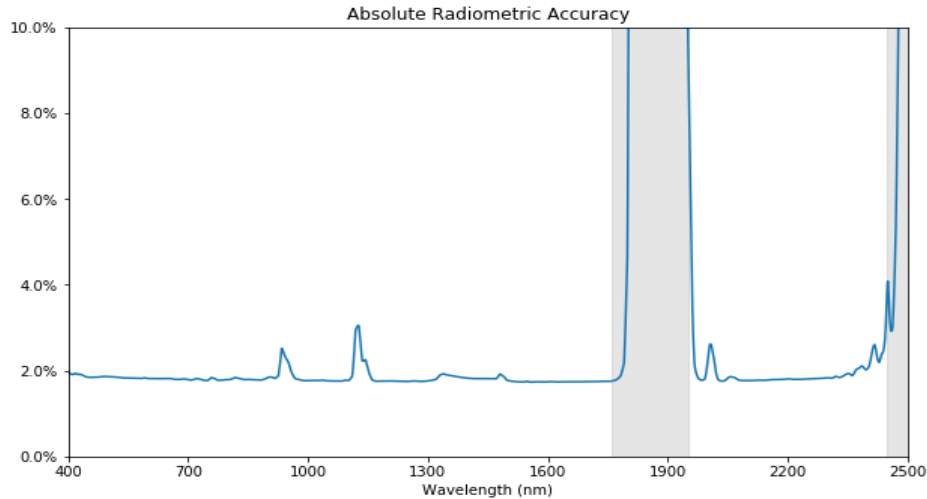


Figure 11. Absolute Radiometric Accuracy

#### 4.5 Line of sight stability

Another crucial parameter is the line of sight (LOS) stability of the instrument with respect to the star tracker, as the instrument has very stringed LOS stability requirements. The instrument LOS stability was analyzed by a STOP analysis considering also platform effects. The STOP analysis is supported by correlations with CME/CTE test data of a representative CFRP structure sample. The results are shown in figure 12 for the RY (ALT) LOS changes. As the instrument shows the biggest LOS changes around the y-axis.

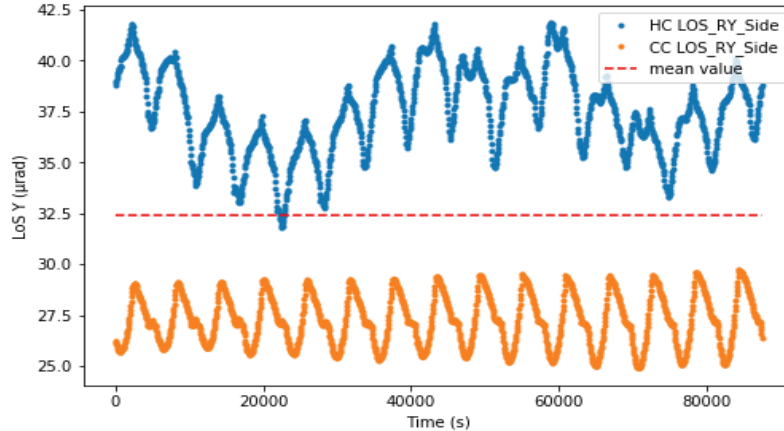


Figure 12. Line of Sight stability evolution over 15 orbits

The figure shows exemplarily the evolution of the LOS of one of the side SU over 15 orbits for the hot case (HC) and the cold case (CC), respectively. These  $3\sigma$  values include a margin factor of 2.5. The red dotted line shows the mean value. The fast oscillations in the graph correspond to the LOS changes during one orbit caused by the temperature changes over the orbit. The additional slow oscillations, which only occur for the HC, are caused by platform effects. The simulation shows a worst-case deviation of the LOS from the mean value over one season of  $9 \mu\text{rad}$ , proving the high stability of the CFRP torus concept of the instrument structure. The variations over one orbit is considerably smaller.

## 5. INSTRUMENT CALIBRATION

### 5.1 Absolute Radiometric Calibration

Absolute radiometric calibration in-orbit is afforded by a sun diffuser. The concept of a sun diffuser is well established for Earth Surface Observing Satellites, like Sentinel 2, EnMAP, or MERIS/OLCI.

The sun is considered – in the spectral range and spectral resolution of CHIME – a well-known source of temporally and spectrally constant irradiance. As the sun’s radiance is orders of magnitude above the instrument sizing earth radiance, and the angular size of the sun does not cover the CHIME field, a calibrated diffuser panel of aperture filling size is placed before the instrument telescope optics relaying the sun light for use as a radiance standard. The diffuser calibration radiance is given by:

$$L_{diff} = \cos(\theta_{Sun})BRDF(\theta_{Sun}, \Phi_{Sun}, \theta_{obs}, \Phi_{obs}, \lambda) * E_{Sun}(\lambda)$$

Sun incidence ( $\theta_{Sun}$ ,  $\Phi_{Sun}$ ) and observation angles ( $\theta_{obs}$ ,  $\Phi_{obs}$ ) are measured with respect to the diffuser normal here. For an ideal Lambertian diffuser, the BRDF has a constant value of  $1/\pi$  ( $sr^{-1}$ ). The deviation from ideal Lambertian behaviour is however significant enough to require an on-ground calibration of the diffuser properties for different incidence and field angles. The Spectralon diffuser angle dependent reflection property (expressed via BRDF), is approximately constant in time, and any degradation can be assessed by using direct lunar observation to provide a radiometric monitoring for the centre field position.

As the diffuser shall calibrate the entire optical path, a mechanism is used to switch between open beam position, and sun diffuser position (see figure 3 - FADE).

The full aperture diffuser is rotated into the optical beam by a door-like mechanism that is built into the instrument’s front cover panel (see figure 3 on the left). It has three positions: earth observation (open, diffuser securely covered), closed (during launch and instrument safe mode, diffuser facing instrument-inward) and solar calibration (diffuser deployed outside the spacecraft reflecting the sun towards telescope mirror TM1). A similar approach is in use on ESA’s Sentinel-2.

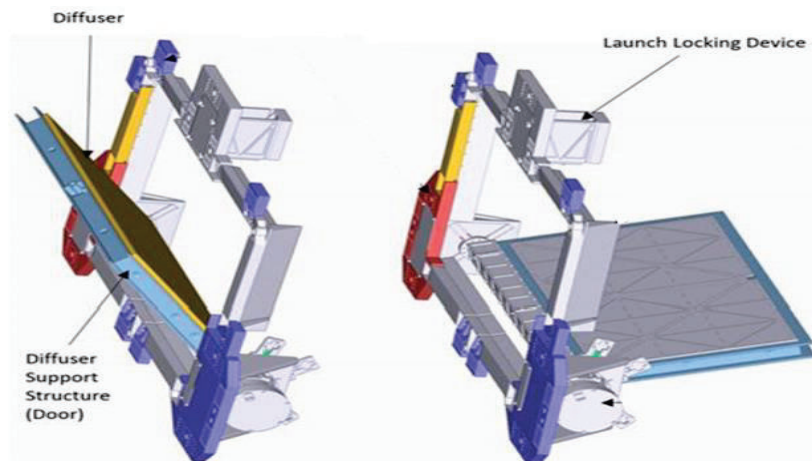


Figure 13. CHIME HSI full aperture diffuser deployment mechanism (FADE). Left: sun-calibration position, right: earth observation. During launch the door is held shut by a launch lock device (top)

The full aperture diffuser has a second use: it doubles as light source for the spectral calibration of the instrument (next section).

## 5.2 Spectral Calibration (on board)

The initial spectral calibration of the CHIME HSI is performed on ground using dedicated optical ground support equipment. To allow a traceability between the on-ground calibration measurements and in-orbit performance the following approach is used:

The On-board spectral calibration is realized via a rare-earth ion doped glass filter (NIST SRM2035) inserted into the normal optical path by a dedicated mechanism during calibration.

The NIST Standard Reference Material SRM2035 [7] is the 3<sup>rd</sup> generation of a well-established and robust filter standard with a mixture of four rare-earth ions: Nd, Yb, Sm, and Ho. It covers the wavelength range from 0.3 to 2.0 micron. Extensive heritage in spectroscopy and the literature is available.

A similar approach using the same rare-earth ion doped glass filters in transmission has been already presented in the literature and used on several missions, most notably JAXA's HISUI hyperspectral instrument [8] and ESA's APEX airborne hyperspectral instrument.

So far, these missions and instruments have used an artificial light source (e.g. tungsten lamp) to illuminate the filter glass. We here present a novel approach utilizing the already existing absolute radiometric calibration light source (the sun irradiance reflected via the diffusor in the FOV of the instrument) that is present on board in front of the telescope:

The concept is shown in figure 14. White light of the sun diffusor (provided by the FADE that used without filter for absolute radiometric calibration) traverses the glass filters which imprint their absorption features onto the light. The filters are built into the Internal Calibration Switching Unit (ICS) and positioned in front of the spectrometer slits during calibration. Since the spectral calibration of the detector pixel grid is not influenced by the front-end telescope, it is sufficient to inject the spectral calibration light before the spectrometers slits (see figure 15).

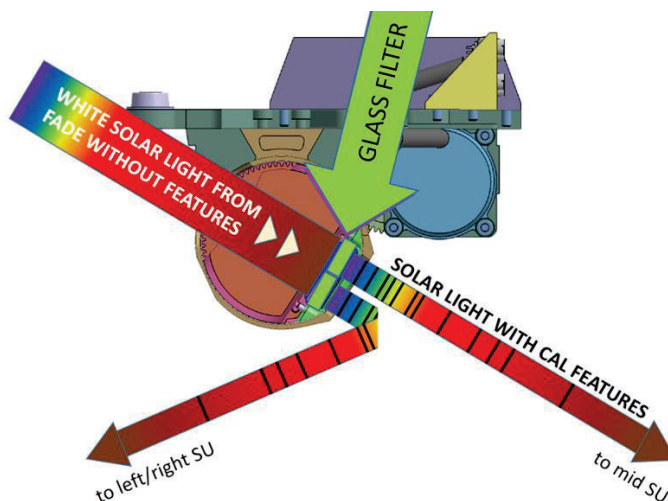


Figure 14. Conceptual sketch of the spectral calibration using sun light afforded by the FADE and rare earth glass filters in front of the spectrometer's slits.

The glass filters are the only additional optical elements that are present in the optical train during calibration. This results in equal and homogeneous (pupil) illumination during spectral calibration.

The filters are built into a rotating drum mechanism making the unit extremely compact. This rotating drum-mechanism is shown in Figures 16-17. The offset and overlapping position of the three filters (shown in turquoise) corresponds to the position of the three slits of the three spectrometers. Depending on the observation mode the ICS rotates to one of

three positions which are shown in Figure 17: (1) in calibration position the glass filters are placed in the optical path for spectral calibration, (2) in close position the optical path is blocked for dark acquisitions, (3) in open position the light passes freely for nominal operation.

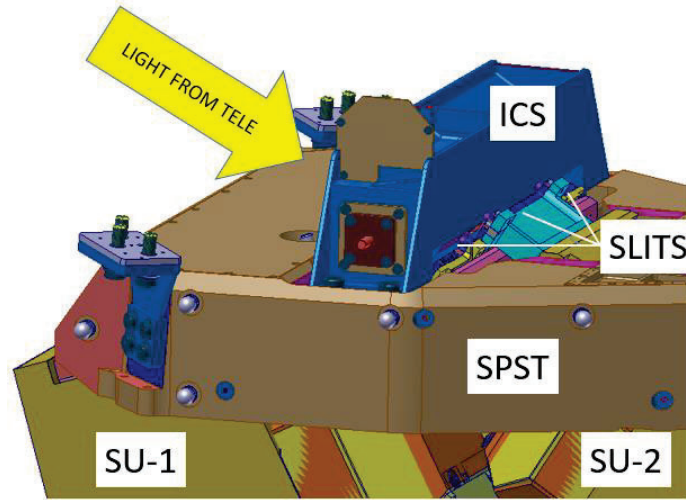


Figure 15. ICS (blue) located in front of the spectrometer slits on top of the spectrometer structure (SPST, brown)

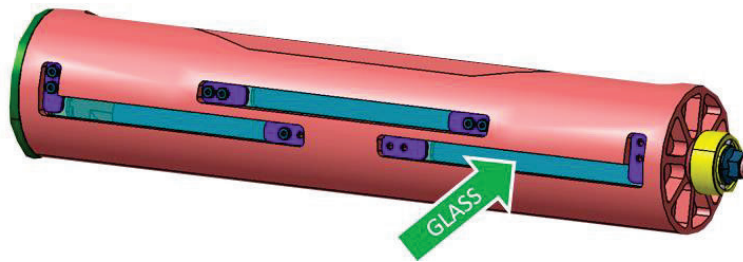


Figure 16. ICS rotating drum part (located in the blue housing in figure 15) with integrated glass filters

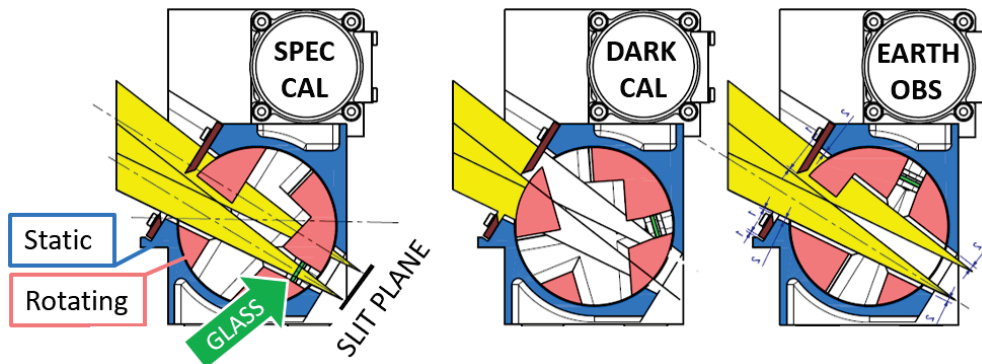


Figure 17. ICS in three positions: calibration (left), close (middle), and open (right). Yellow: optical light path with light entering the ICS from the upper left and the focal plane on the lower right. The glass filters are shown in green.



The spectral calibration will be performed in direct sequence with the radiometric sun calibration since the diffuser is already in sun position to minimize overhead.

### Spectral Calibration principle

The calibration principle of the ICS is to observe the absorption features of the glass filters (NIST Standard Reference Material (SRM) 2035b) in-orbit and to match the features to their well characterized reference wavelengths (Ion-absorption lines) to map the spectral positions on the detector and compare with the on-ground reference calibration.

Three measurements are needed to accomplish this:

- a sun observation  $SO(\lambda)$ ,
- a sun observation with the glass filters deployed  $SFO(\lambda)$ ,
- a reference transmission of the glass filters  $FR(\lambda)$ .

Only the  $SO(\lambda)$  and the  $SFO(\lambda)$  are acquired within the on-board calibration and are shown in Figure 18. The former signal is acquired with the FADE in “sun calibration” position and the ICS in “open” (=Earth observation, no filter in the light path) position. The latter signal is recorded with the FADE in “sun calibration” position and the ICS in “calibration” (=glass-filters deployed) position. The observed filter glass transmission  $FO(\lambda)$  containing the absorption features are retrieved by division of  $SFO(\lambda)$  by  $SO(\lambda)$ , which eliminates all features related to the spectrum of the sun:  $FO(\lambda)=SFO(\lambda)SO(\lambda)$ .

A typical  $FO$  curve is shown in Figure 19. By matching the prominent absorption features of the  $FO(\lambda)$  to their respective counterparts in the  $FR(\lambda)$ , spectral shifts can be detected. A linear correction using at a minimum two spectral features at least 100 nm apart is sufficient for the grating spectrometer, which has an intrinsic linear dispersion (Note: any non-linearity is constrained by distortions of the last mirror of the spectrometers and can be assumed stable during the mission). The spectral calibration with the glass filters is considered absolute. Any degradation during launch can be detected by comparison with oxygen absorption lines performed during commissioning.

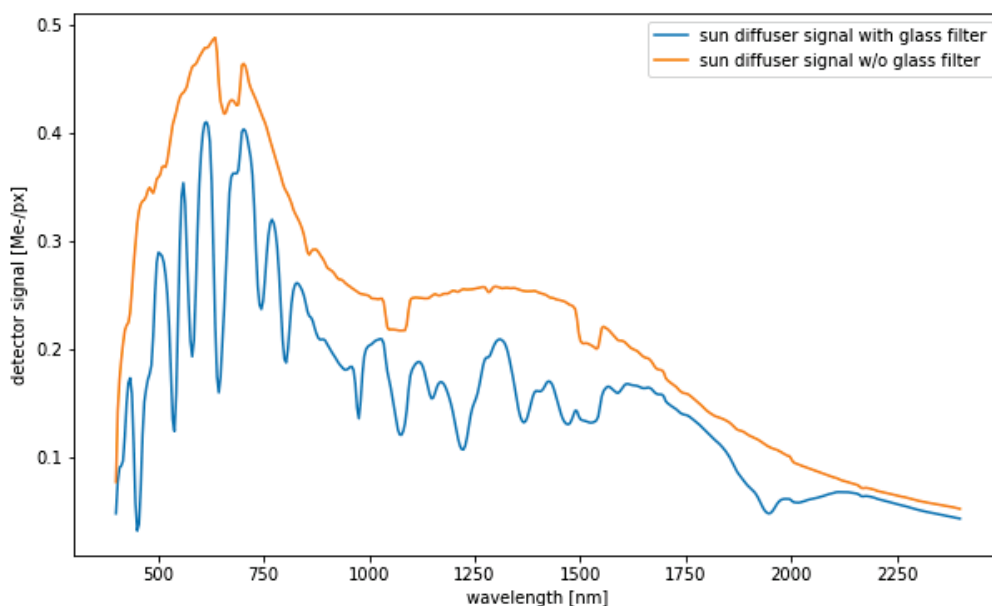


Figure 18. Comparison between typical signals from a sun observation via the FADE with (SFO) and without (SO) the glass filter deployed.

The signal is biased by the of sun irradiance as the sun signal is not constant for all CHIME spectral channels. Sun diffusor reference measurements without spectral calibration source allow the simple reconstruction of the glass filter transmission as shown in figure 19.

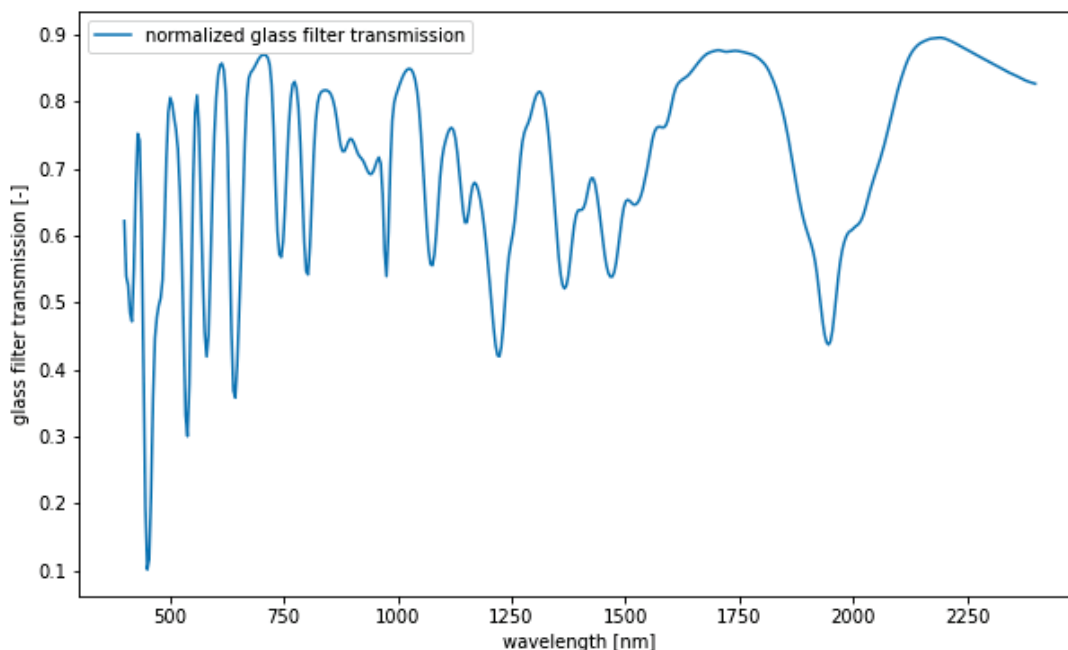


Figure 19. Observed filter glass transmission (FO) containing absorption features used for spectral calibration and retrieved by division of signals in Figure

To allow a traceability between the on-ground calibration and in-orbit performance, the filter glass is on ground illuminated by an integrating sphere with a white light source. The -on-ground illumination condition are different from the conditions in orbit in two ways:

- Illumination happens via white light instead of sun light
- Direct illumination of the filter glass instead of illumination through sun diffuser.

The filter glass has been positively assessed in ESA ESTEC Radiation test facility for radiation levels (plus safety margin) present for the CHIME mission.

During the commissioning phase the performance of the algorithm can be tested with the on ground test data with a high level of confidence allowing a traceability between on-ground spectral calibration and in-orbit performance.

The reconstructed normalized glass filter transmission will be used as input for the spectral calibration processor provided by VITO. Assessments show that the calibration accuracy fully satisfies the performance accuracy needs.

## 6. INSTRUMENT PARTNERS AND SUBCONTRACTORS

The CHIME HSI instrument described in this paper is built by a consortium of Companies from Europe under the lead of OHB System AG, Germany under the System and Mission Prime Thales Alenia Space, France. The table below lists the respective Partners and their contributions.

Table 3. CHIME Instrument Partners

Predevelopment / Aspect	Partner	Country
System and Mission Prime	Thales Alenia Space	France
Structure & Optical Bench	INVENT	Germany
Mirrors	LEONADO/TSESO	Italy / France
Spectrometer Subsystem, Slit, Grating	AMOS	Belgium
Focal Plane System	LEONARDO	Italy
Order Sorting Filter	Optics Balzer	Germany
Detector	Teledyne-e2v	UK
Full aperture diffusor	AVS	Spain
Focal plane radiator	IberEspacio	Spain
MLI	FHP	Portugal
Refocusing Mechanism	Sener	Spain
Instrument Control Unit	DSI	Germany
Instrument Power Unit	Sitael	Italy
Calibration Processor; Vicarious Calibration	VITO	Belgium
Ground Calibration & Characterization	LEONARDO	Italy

## 7. CONCLUSION / OUTLOOK

We have presented an overview of the CHIME Hyperspectral Imager Design at the state of the Preliminary Design Review. The HSI design is adequately consolidated for PDR and the projected/calculated performance is high with good margin in many areas.

The innovative architecture presented in the last paper was improved and led to a robust design also thanks to the knowledge and heritage available in the consortium. The open and modular design has shown to be very helpful in many areas, most notably AIT planning but also in a very good understanding of performance contributors and budgets. With the updated spectral calibration mechanism, we have presented a robust innovation in the area of spectral calibration combining two well know calibration schemes. The refined design combination of compact metal backend and well controlled CFRP-Zerodur front-end exceeds the initial performance predictions creating a very stable instrument. In future papers further design refinements and AIT and performance measurement results will be provided.

## 8. ACKNOWLEDGMENTS

The CHIME Phase B2CDE1 contract is carried out as part of the Copernicus Programme, which is funded by the EU and ESA.

The authors thank the overall CHIME industrial team at OHB (DE) with the partners at TAS (FR), AMOS (BE), LEONARDO (IT), INVENT (DE), OBJ (DE), Te2v (UK), TSESO (FR), DSI (DE), Sener (ES), Sitael (IT), IberEspacio (ES), VITO (BE), FHP (PT), and AVS (ES). Further, we acknowledge the steady contribution and effort of our colleagues at ESA-ESTEC (The Netherlands), ESA-ESOC (Germany), ESA-ESRIN (Italy) and the CHIME Mission Advisory Group (MAG) for actively supporting the missions.

## REFERENCES

- [1] Chabrilat, S., K. Segl, S. Foerster, M. Brell, L. Guanter, A. Schickling, S. Fischer, T. Storch, H.-P. Honold, EnMAP Pre-Launch and Start Phase: Mission Update, IGARSS Conference Proceedings (2022)
- [2] Lopinto, E., L. Fasano, F. Longo, P. Sacco, Current Status of PRISMA Mission, IGARSS Conference Proceedings (2022)
- [3] Celesti M., M. Rast, V. Boccia, F. Gascon, C. Isola, J. Nieke, J. Adams, The Copernicus Hyperspectral Imaging Mission for the Environment (CHIME): Status and Planning, IGARSS Conference Proceedings (2022)
- [4] Rast, M.; et al., “Copernicus Hyperspectral Imaging Mission Requirements Document” ESA-EOPSM-CHIM-MRD-3216, version 3.0; [https://esamultimedia.esa.int/docs/EarthObservation/Copernicus\\_CHIME\\_MRD\\_v3.0\\_Issued\\_21\\_01\\_2021.pdf](https://esamultimedia.esa.int/docs/EarthObservation/Copernicus_CHIME_MRD_v3.0_Issued_21_01_2021.pdf) (2021)
- [5] Buschkamp P. et al. “CHIME’s hyperspectral imaging spectrometer design result from phase A/B1”; Proc. SPIE 11852, International Conference on Space Optics — ICSO (2020)
- [6] Renotte E.; et al.; “The Dual-blazed Diffraction Grating of the CHIME Hyperspectral Instrument: design, modelling & breadboarding” ICSO (2022)
- [7] Choquette S, Travis J. and Duewer D. "SRM 2035: a rare-earth oxide glass for the wavelength calibration of near-infrared dispersive and Fourier transform spectrometers", Proc. SPIE 3425, Optical Diagnostic Methods for Inorganic Transmissive Materials 1998
- [8] Tatsumi K. et al., "Retrieval of spectral response functions for the hyperspectral sensor of HISUI (Hyperspectral Imager SUIt) by means of onboard calibration sources." *Proc. SPIE 8176, Sensors, Systems, and Next-Generation Satellites XV, 81760S (3 October 2011)*